

Materials by Design: Using Architecture and Nanomaterial Size Effects to Attain Unexplored Properties

Julia R. Greer

Julia R. Greer is a professor of materials science, mechanics, and medical engineering in the Division of Engineering and Applied Sciences at the California Institute of Technology.

Engineers are actively trying to mimic hard biomaterials such as mollusk shells and beaks because of their resilience and damage tolerance, which are believed to stem from hierarchical arrangements in their design. Technological advances in fabrication methods make it possible to create architected structural metamaterials using materials whose design and dimensionality are similar to those found in nature and whose hierarchical ordering ranges from angstroms and nanometers at the level of material microstructure to microns and millimeters at the level of macroscale architecture.

The use of architectural features in defining multidimensional material design space will enable the independent manipulation of coupled physical attributes and the development of materials with unprecedented capabilities. The result is that the behavior and properties of architected structural metamaterials can no longer be defined solely by the properties of the constituent solid or by the structure or architecture; instead they benefit from the linked behavior of the material and the structure at very small dimensions. The material creation paradigm will shift from *structure* → *processing* → *property* to *property* → *architecture* → *fabrication*.

The feasibility of this “materials by design” approach is gated by the ability to understand and predict the mechanical responses of metamaterials, whose properties are controlled by engineered structure in addition to atomic composition, and whose feature size and geometry are critical design parameters. Current research is making significant headway testing, demonstrating, and understanding these properties.

Introduction

The concept of architecture in the design of materials is common in nature. For example, the properties of butterfly wings are a function of their multiscale, hierarchical construction. The nanoarchitecture of a butterfly wing interacts with light to create multicolored wings, and for shells such as nacre small ceramic platelets are key to their extreme resilience (Von Freymann et al. 2013). Many research groups have attempted to mimic and replicate the properties of these and other natural materials.

Hierarchically designed cellular materials have been used for many decades as the basis for mechanically robust engineered structures, such as the Eiffel Tower. The introduction of architectural elements enables the creation of structures that are both lightweight, because they use a fraction of monolithic material with the same dimensions, and strong, because the architecture provides a way to more efficiently distribute load-carrying capability.

Nanoarchitected structural metamaterials extend the concept of architecture to the micro- and nanometer length scale, often down to the atomistic level of material microstructure, enabling the use of material size effects to create metamaterials with amplified properties. Size effects that emerge in solids at the nanoscale—single crystalline metals become stronger, nanocrystalline metals become weaker, and metallic glasses and ceramics undergo brittle-to-ductile transition (Greer and De Hosson 2011)—can be exploited by using micron- to nanometer-scale building blocks to create larger structures.

Structural Metamaterials: Manipulation of Cellular Properties

The mechanical performance of architected solids on the macroscale is a function of their deformation mechanism, relative density, and constituent material properties (Deshpande and Fleck 2001; Fleck et al. 2010; Gibson and Ashby 1997; Meza et al. 2014; Ng et al. 2009; Schaedler et al. 2011; Valdevit et al. 2013; Wadley et al. 2003). Cellular solids offer a useful combination of light weight and mechanical integrity and have been studied at the macroscale experimentally, computationally, and theoretically. All of these studies assume that material properties of the constituent solid are constant and geometry is the

single tunable parameter (Fleck and Qiu 2007; Fleck et al. 2010; Hutchinson and Fleck 2006; Symons and Fleck 2008).

Cellular solids can deform by either bending or stretching of the elements, both of which are dictated by lattice geometry and its nodal connectivity (Sun et al. 2013; Wang et al. 2003). A three-dimensional (3D) structure must have a connectivity of $Z = 6$ at the nodes to be rigid; a connectivity of $Z = 12$ to be stretching-dominated, which leads to the stiffest materials; and a connectivity of $6 \leq Z < 12$ to be bending-dominated, which results in more compliant materials (Wang et al. 2003).

The structural deformation mechanism, determined by the nodal connectivity, directly affects the stiffness and yield strength of the overall structure (Deshpande et al. 2001a,b). The yield strength and stiffness of 3D open-cell bending-dominated structures, such as honeycombs, scale as $\sigma_y = 0.3\bar{\rho}^{1.5}\sigma_{ys}$ and $E = \bar{\rho}^2 E_s$, where σ_{ys} and E_s are the yield strength and modulus of the constituent solid (Gibson and Ashby 1997). For 3D stretching-dominated structures, such as the octet truss, the yield strength and modulus scale as $\sigma_y = 0.3\bar{\rho}\sigma_{ys}$ and $E = 0.3\bar{\rho}E_s$, causing strength to decrease less rapidly (compared to bending-dominated structures) as relative density decreases.

Relative densities of cellular solids, along with stiffness and strength, can be modulated by using hollow tubes instead of solid rods in the same architecture or by creating hierarchical structures (figure 1). When hollow tubes are used in low-density cellular solids, structural effects can be activated by changing the various ratios of geometric parameters that define the lattice tubes. For example, reducing the slenderness ratio from 1 to 20 causes a 2 order-of-magnitude reduction in relative density, and hollowing out the tubes reduces density by an additional order of magnitude. Replacing solid beams with self-similar, fractal-like elements gives a further 1.5 to 2 order-of-magnitude reduction in density.

Demonstrated Improvements in Mechanical Behavior

Recent work in our research group demonstrated the attainment of simultaneous light weight, high strength/stiffness, and recoverability by combining the architecture and material size effect of nanomaterials. We tested the mechanical behavior of octet alumina nanolattices, a class of new, lightweight durable materials that have optimized nano-sized induced material properties, high surface area, and 3D architectures and are desperately needed for a variety of applications (e.g., small-scale energy storage devices, biomedical devices, space travel vehicles, wind turbines, personnel protection, and lightweight thermal insulation).

One way to think about such nanolattices is a 2D nanoribbon wrapped around a 3D architecture (figure 2). Ordered cellular solids such as the octet truss and kagome lattice have robust mechanical properties such as a combination of high strength and fracture toughness (Deshpande et al. 2001a,b). The geometry of these structures makes it possible to create materials with not only improved mechanical properties but also low densities and high surface area to volume ratios.

We found that they contain ~99 percent air recovered after compression of more than 50 percent (Jang et al. 2013; Meza and Greer 2014; Meza et al. 2014, 2015; Montemayor et al. 2014). Hollow rigid nanolattices have recently attracted much interest as they attained GPa-level stiffnesses at ~10 percent of the density of the parent solid (Jang et al. 2013; Meza and Greer 2014; Meza et al. 2014, 2015; Montemayor et al. 2014). At some critical wall thickness nearly all nanotrusses—ceramic, metallic, and metallic glass—fully recovered after <50 percent compression without sacrifice in strength. Our most recent work demonstrated that these nanolattices also exhibit insensitivity to flaws, i.e., failure tolerance (Montemayor et al. 2015).

All of these developments position scientists favorably to address the challenge of developing lightweight and damage-tolerant materials that can have a suite of other valuable properties, such as thermal insulation (conductivity), as well as electronic and optical response.

Fabrication

Significant efforts are under way to develop architected materials with precisely designed (i.e., nonstochastic) geometries, which can support the prototyping of exceptionally lightweight, strong, and tough metamaterials. Control of such nanolattice geometries has been made possible by advances in 3D

micro- and nanofabrication techniques, ranging from polymer waveguides to microstereolithography to direct laser writing two-photon lithography (DLW TPL) (Zheng et al. 2014).

Direct Laser Writing Two-Photon Lithography (DLW TPL)

Advantages of the TPL method over other 3D fabrication techniques are precise nanometer and submicron feature resolution, smooth beam surfaces, and extreme versatility in geometry (Fischer and Wegener 2013; Sun and Kawata 2004; Xiong et al. 2012). Nanolattices fabricated by TPL enable a reduction in size by up to 3 orders of magnitude compared to microlattices fabricated by 3D printing or by self-propagating polymer waveguides, and they are amenable to subsequent coating and scaffold removal. Their appearance is monolithic and may resemble an iridescent aerogel whose strength is comparable to that of metals and ceramics.

The individual building blocks that constitute nanolattices have dimensions that are below the resolution of the human eye, with strut lengths of 3–20 μm , diameters of 100 nm–1 μm , and wall thicknesses of 5–600 nm (Jacobsen et al. 2007; Jang et al. 2013; Meza and Greer 2014; Meza et al. 2014, 2015; Montemayor et al. 2014, 2015). Their useful properties arise from a combination of size-dependent nanomaterial properties and structural response of the discrete architecture; they cannot be predicted solely by scale-free continuum theories (Gibson and Ashby 1997; Torrents et al. 2012; Valdevit et al. 2013).

Figure 3 shows a schematic representation of the fabrication steps during the nanolattice creation procedure. Nanolattices were first fabricated from a negative photoresist (IP-Dip 780) using DLW TPL, which uses a 780 nm femtosecond pulsed laser focused into a small volume element, a voxel, in the polymer. The energy is sufficient to cross-link the monomer and to harden the material within the voxel before the two photons are absorbed. The elliptical voxel is rastered in three dimensions in a droplet of photoresist to effectively sculpt the prescribed structure, which can have virtually any geometry; some examples are shown in figures 1, 2, and 4.

Other Methods

To make nanolattices out of different materials, the polymer scaffolds are coated (as conformally as possible) with the specific material of interest (e.g., metals, semiconductors, oxides, metallic glasses, piezoelectric materials, other polymers). We have demonstrated the feasibility of sputtering different metals onto nanolattices up to ~ 300 nm (Montemayor et al. 2014; Montemayor and Greer 2015); and Meza and colleagues and several other research groups successfully utilized atomic layer deposition to apply ~ 5 –60-nm-thick ceramic alumina (Al_2O_3) and titanium nitride (TiN) coatings onto polymer scaffolds (Jang et al. 2013). After deposition, the original internal polymer scaffold is exposed by slicing two of the six sides off the sample using a focused ion beam and then removed using an oxygen plasma, revealing a hollow-tube nanolattice that is made entirely of the coating material (Meza and Greer 2014; Meza et al. 2014, 2015; Montemayor and Greer 2015; Montemayor et al. 2014, 2015).

Demonstration of Enhanced Properties

Hollow Nanolattices

Our group has demonstrated that hollow Al_2O_3 nanolattices with octet truss geometry and relative densities of $\rho = 10^{-4} - 10^{-1}$ recovered up to 98 percent of their initial height after uniaxial compressions in excess of 50 percent (Jang et al. 2013; Meza and Greer 2014; Meza et al. 2014, 2015). Their ductile-like deformation and recoverability were attributed to the critical ratio between the wall thickness (t) and the semimajor axis (a) of the hollow elliptical strut cross section. When (t/a) is less than the critical value (~ 0.03 for alumina), the nanolattices deformed via shell buckling and recovered after deformation; at greater (t/a) values, they failed catastrophically with little to no recovery (Meza and Greer 2014; Meza et al. 2014).

The constituent Al_2O_3 is a brittle ceramic; reducing the wall thickness to the nanometer level and “wrapping” the film around a 3D architecture enables the metamaterial to bypass the properties of the constituent solid and to exhibit a diametrically opposite property, recoverability. The ~ 10 nm thickness reduces the number and size of flaws in the Al_2O_3 —the largest is only 10 nm! The combination of

Weibull statistics flaw distribution-based fracture, a material size effect, and structural deformation mechanism as a function of (t/a) makes it possible for ceramic nanolattices to have such unique properties (Jang et al. 2013; Meza and Greer 2014; Meza et al. 2014, 2015).

Solid Nanolattices

The enhanced properties induced by the interplay of structural and material size effects have also been observed in TPL-created lattices with solid metal struts (Blanco et al. 2000). Copper (Cu) mesolattices were created using an inverse DLW TPL method: a negative of the scaffold was patterned in a positive-tone resist, and then Cu was electroplated into the exposed pores (Blanco et al. 2000). Removal of the polymer mold revealed a free-standing mesolattice with solid Cu beams whose thickness and grain size were $\sim 2 \mu\text{m}$. These mesolattices had relative densities between 40 percent and 80 percent and a unit cell of $6 \mu\text{m}$ and $8 \mu\text{m}$, and at the highest density their compressive yield strength was $\sim 330 \text{ MPa}$, which is a factor of ~ 2.5 higher than that of bulk copper, 133 MPa .

This amplification in strength is a result of the size effect in single crystalline metals (“smaller is stronger”) (Blanco et al. 2000). These results imply that the architected Cu nanolattices outperformed bulk copper by a factor of ~ 3 for relative densities of $\rho > 0.6$ —that is, when more than 40 percent of the material was removed from a monolithic cube of the same volume.

Other Structures and Materials

Current pursuits in the field of architected structural metamaterials include efforts to develop auxetic 3D structures (i.e., materials with a negative Poisson’s ratio), which are fabricated using DLW TPL (Babae et al. 2013; Lee et al. 2012). Typical monolithic materials expand in the direction orthogonal to the loading axis when uniaxially compressed, whereas auxetic materials contract in this direction.

Pentamode materials, or 3D solids that ideally behave as fluids, have also been designed and fabricated using TPL and provide a pathway to decouple bulk and shear moduli, enabling independent wave propagation through media (Rinne et al. 2007).

Challenges of Scalability

The most significant obstacle to incorporating structural nanoarchitected metamaterials in useful technological applications is scalability, that is, the ability to manufacture either a large number of small-scale components or materials with large dimensions in a reasonable amount of time. Stochastic foams (e.g., nanoporous gold), in which the porosity distribution is random, have been explored as a possible vehicle for propagating material size effects to larger scales (Hodge et al. 2005). But these foams exhibit poor scaling of strength with relative density and are ultimately limited in the types of architecture they can create (Fleck et al. 2010).

Some technologies that could lead to scalability are roll-to-roll fabrication with nanoimprintable patterns, holographic lithography, and phase-shifting masks.

Outlook

This selective overview highlights the state of the art of some structural metamaterials with dimensions that span microns to nanometers. Experiments on nanolattices have demonstrated that unique material size effects that emerge only at the nanoscale can be effectively propagated to macroscopic dimensions and have the potential to create new classes of bulk engineered materials with unprecedented properties.

Nanoarchitected metamaterials represent a new approach to “materials by design,” making it possible to create materials with previously unattainable combinations of properties—light weight and enhanced mechanical performance—as well as unique thermal, optical, acoustic, and electronic attributes. Some realistic technological advances enabled by these metamaterials are untearable and unwettable paper, tunable filters and laser sources, tissue implants generated on biodegradable scaffolds that can be implanted and absorbed by the human body, battery-powered implantable chemical sensors, and extremely insulating and super-thin thermal lining for jackets and sleeping bags.

References

- Babae S, Shim J, Weaver JC, Chen ER, Patel N, Bertoldi K. 2013. 3D soft metamaterials with negative Poisson's ratio. *Advanced Materials* 25(36):5044–5049.
- Blanco A, Chomski E, Gratchak S, Ibisate M, John S, Leonard SW, Lopez C, Meseguer F, Miguez H, Mondia JP, and 3 others. 2000. Large-scale synthesis of a silicon photonic crystal with a complete three-dimensional bandgap near 1.5 micrometres. *Nature* 405:437–440.
- Chiras S, Mumm DR, Evans AG, Wicks N, Hutchinson JW, Dharmasena K, Wadley HNG, Fichter S. 2002. The structural performance of near-optimized truss core panels. *International Journal of Solids and Structures* 39:4093–4115.
- Deshpande VS, Fleck NA. 2001. Collapse of truss core sandwich beams in 3-point bending. *International Journal of Solids and Structures* 38:6275–6305.
- Deshpande VS, Ashby MF, Fleck NA. 2001a. Foam topology: Bending versus stretching dominated architectures. *Acta Materialia* 49:1035–1040.
- Deshpande VS, Fleck NA, Ashby MF. 2001b. Effective properties of the octet-truss lattice material. *Journal of the Mechanics and Physics of Solids* 49(8):1747–1769.
- Fischer J, Wegener M. 2013. Three-dimensional optical laser lithography beyond the diffraction limit. *Laser and Photonics Reviews* 7(1):22–44.
- Fleck NA, Qiu X. 2007. The damage tolerance of elastic-brittle, two-dimensional isotropic lattices. *Journal of the Mechanics and Physics of Solids* 55:562–588.
- Fleck NA, Deshpande VS, Ashby MF. 2010. Micro-architected materials: Past, present and future. *Proceedings of the Royal Society A: Mathematical, Physical and Engineering Science* 466:2495–2516.
- Gibson LJ, Ashby MF. 1997. *Cellular solids: Structure and properties*. Cambridge, UK: Cambridge University Press.
- Greer JR, De Hosson JTM. 2011. Plasticity in small-sized metallic systems: Intrinsic versus extrinsic size effect. *Progress in Materials Science* 56:654–724.
- Hodge AM, Biener J, Hsiung LL, Wang YM, Hamza AV, Satcher JH. 2005. Monolithic nanocrystalline Au fabricated by the compaction of nanoscale foam. *Journal of Materials Research* 20:554–557.
- Hodge AM, Biener J, Hayes JR, Bythrow PM, Volkert CA, Hamza AV. 2007. Scaling equation for yield strength of nanoporous open-cell foams. *Acta Materialia* 55:1343–1349.
- Hutchinson RG, Fleck NA. 2006. The structural performance of the periodic truss. *Journal of the Mechanics and Physics of Solids* 54:756–782.
- Jacobsen AJ, Barvosa-Carter W, Nutt S. 2007. Micro-scale truss structures formed from self-propagating photopolymer waveguides. *Advanced Materials* 19(22):3892–3896.
- Jang D, Meza LR, Greer F, Greer JR. 2013. Fabrication and deformation of three-dimensional hollow ceramic nanostructures. *Nature materials* 12:893–898.
- Lee J-H, Singer JP, Thomas EL. 2012. Micro-/nanostructured mechanical metamaterials. *Advanced Materials* 24(36):4782–4810.
- Meza LR, Greer JR. 2014. Mechanical characterization of hollow ceramic nanolattices. *Journal of Materials Science* 49(6):2496–2508.
- Meza LR, Das S, Greer JR. 2014. Strong, lightweight, and recoverable three-dimensional ceramic nanolattices. *Science* 345:1322–1326.
- Meza L, Zelhofer AJ, Clarke N, Mateos AJ, Kochmann DM, Greer JR. 2015. Resilient 3D hierarchical architected metamaterials. *Proceedings of the National Academy of Sciences* 112(37):11502–11507.
- Montemayor LC, Meza LR, Greer JR. 2014. Design and fabrication of hollow rigid nanolattices via two-photon lithography. *Advanced Engineering Materials* 16(2):184–189.
- Montemayor LC, Greer JR. 2015. Mechanical response of hollow metallic nanolattices: Combining structural and material size effects. *Journal of Applied Mechanics* 82(7):071012.
- Montemayor LC, Wong WH, Zhang Y-W, Greer JR. 2015. Insensitivity to flaws leads to damage tolerance in brittle architected meta-materials. *Nature Scientific Reports* (in revision).
- Ng KY, Lin Y, Ngan AHW. 2009. Deformation of anodic aluminum oxide nano-honeycombs during nanoindentation. *Acta Materialia* 57:2710–2720.

- Rinne SA, García-Santamaría F, Braun PV. 2007. Embedded cavities and waveguides in three-dimensional silicon photonic crystals. *Nature Photonics* 2:52–56.
- Schaedler TA, Jacobsen AJ, Torrents A, Sorensen AE, Lian J, Greer JR, Valdevit L, Carter WB. 2011. Ultralight metallic microlattices. *Science* 334:962–965.
- Sun H-B, Kawata S. 2004. Two-photon photopolymerization and 3D lithographic microfabrication. *Advances in Polymer Science*, vol. 170: NMR, 3D Analysis, Photopolymerization. Berlin: Springer-Verlag. pp. 169–273.
- Sun J, Bhushan B, Tong J. 2013. Structural coloration in nature. *RSC Advances* 3(35):14862–14889.
- Symons DD, Fleck NA. 2008. The imperfection sensitivity of isotropic two-dimensional elastic lattices. *Journal of Applied Mechanics* 75(5):051011.
- Torrents A, Schaedler TA, Jacobsen AJ, Carter WB, Valdevit L. 2012. Characterization of nickel-based microlattice materials with structural hierarchy from the nanometer to the millimeter scale. *Acta Materialia* 60:3511–3523.
- Valdevit L, Godfrey SW, Schaedler TA, Jacobsen AJ, Carter WB. 2013. Compressive strength of hollow microlattices: Experimental characterization, modeling, and optimal design. *Journal of Materials Research* 28:2461–2473.
- Von Freymann G, Kitaev V, Lotsch BV, Ozin GA. 2013. Bottom-up assembly of photonic crystals. *Chemical Society Reviews* 42(7):2528–2554.
- Wadley HNG, Fleck NA, Evans AG. 2003. Fabrication and structural performance of periodic cellular metal sandwich structures. *Composites Science and Technology* 63:2331–2343.
- Wallach JC, Gibson LJ. 2001. Mechanical behavior of a three-dimensional truss material. *International Journal of Solids and Structures* 38:7181–7196.
- Wang J, Evans AG, Dharmasena K, Wadley HNG. 2003. On the performance of truss panels with Kagome cores. *International Journal of Solids and Structures* 40:6981–6988.
- Xiong W, Zhou YS, He XN, Gao Y, Mahjouri-Samani M, Jiang L, Baldacchini T, Lu YF. 2012. Simultaneous additive and subtractive three-dimensional nanofabrication using integrated two-photon polymerization and multiphoton ablation. *Light: Science and Applications* 1:e6.
- Zheng X, Lee H, Weisgraber TH, Shusteff M, Deotte JR, Duoss E, Kuntz JD, Biener MM, Kucheyev SO, Ge Q. 2014. Ultra-light, ultra-stiff mechanical metamaterials. *Science* 344:1373–1377.

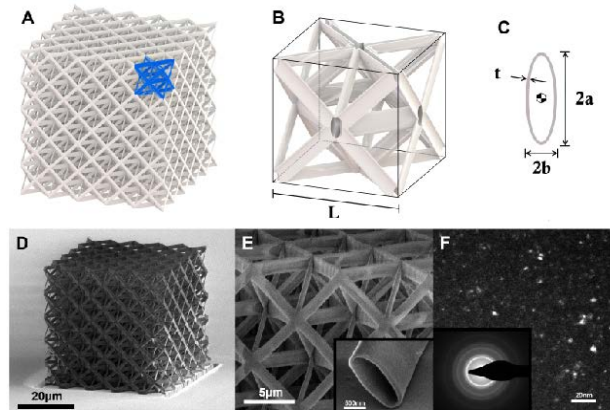


FIGURE 1 Octet truss design. (A) Single unit cell highlighted. (B) Cutaway of hollow octet truss unit cell. (C) Hollow elliptical nanolattice tube. (D) Scanning electron microscope image of alumina nanolattice. (E) Zoomed-in image of (D). (F) Dark field transmission electron microscope image with diffraction pattern: amorphous microstructure. Reprinted with permission from Meza et al. (2014).

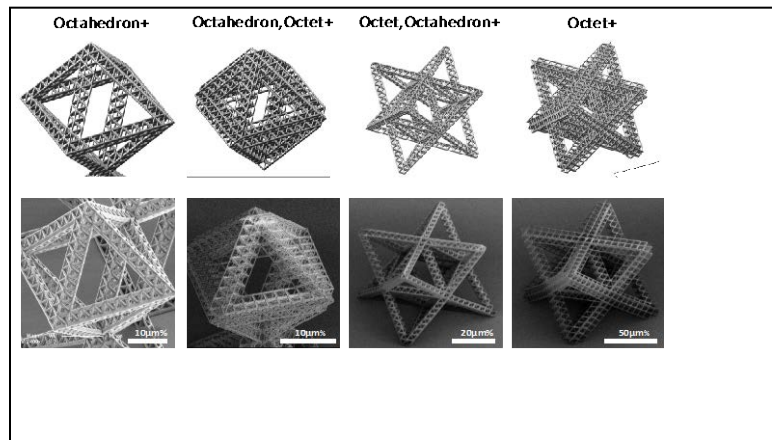


FIGURE 2 Computer-aided designs and scanning electron microscope images of fractal nanotrusses with various geometries specified above each set. Reprinted with permission from Lucas et al. (2015).

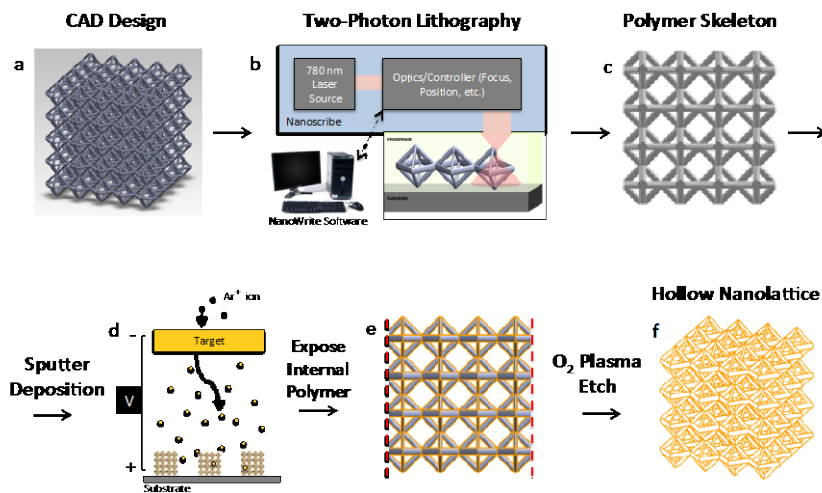


FIGURE 3 A schematic of the two-photon lithography technique followed by the deposition of material of interest and etching out of the internal polymer scaffold. Reprinted with permission from Montemayor et al. (2014).

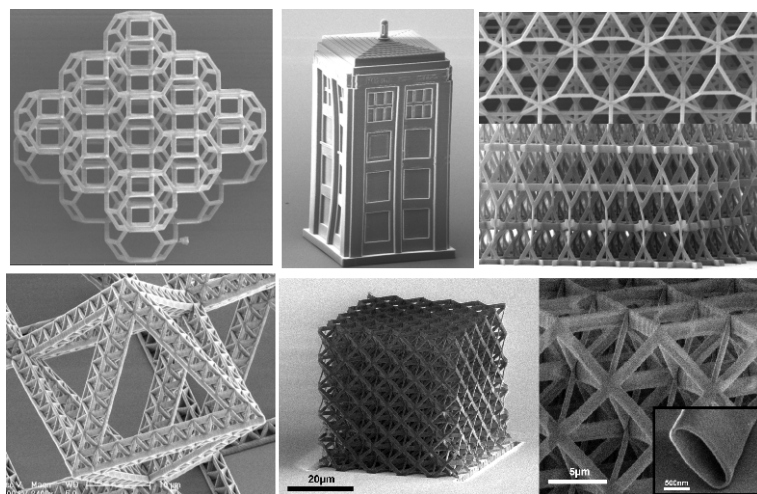


FIGURE 4 Examples of different architectures written by the two-photon lithography technique showing the versatility of this approach. Reprinted with permission from Lucas et al. (2015) (bottom row left) and Meza et al. (2014) (bottom row center and right).